

A numerical study of heterogeneous annealing in a finite one-dimensional geometry

Jeremiah Lethoba¹, Pavel M Bokov² and Pavel A Selyshchev¹

¹Department of Physics, University of Pretoria Private bag X20 Hatfield 0028 South Africa

² The South African Nuclear Energy Corporation (Necsa), Building 1900, P.O. Box 582, Pretoria 0001, South Africa

E-mail: lethoba77@gmail.com, pavel.bokov@necsa.co.za, selyshchev@gmail.com

Abstract. In this paper, a numerical investigation of initiation of thermal annealing of radiation-induced defects in a sample with finite dimensions is performed. The annealing is initiated by means of a thermal pulse that heats the sample to a specific temperature and set depth from its surface. The dependence of the annealing time on the initial defect density and on the parameters of the thermal pulse is studied.

1. Introduction

The irradiation of a material with high-energy particles causes the formation of different types of defects in its crystalline lattice. At any temperature above absolute zero, the defects anneal spontaneously and the rate of annealing increases with temperature. Therefore, in order to anneal crystal defects, the sample must be heated. Usually, the temperature is increased on the surface of the sample and is kept constant for some time [1]. For small samples, transient processes (heating) can be neglected and the temperature distribution can be assumed to be uniform over the sample. For large samples, on the contrary, transient processes can not be neglected and achieving a homogeneous temperature distribution can require considerable time and energy. However, in order to anneal defects throughout the volume of the sample, it is not always necessary to heat the entire sample. It is known that under certain circumstances it is possible to develop a self-propagating annealing similar to an autowave [2, 3]. Its initiation requires significantly less energy, and the annealing occurs in a much shorter time. In this case, the annealing actually takes place near the wave front, in the so-called *annealing zone* (Fig. 1). The annealing zone separates regions of the sample with and without defects and moves into the latter at a constant velocity. In the coordinate system that moves with this velocity, the temperature and defect distributions remain constant over the sample (Fig. 2). The density of defects in the annealing zone falls from its initial value ahead of the wave front to practically zero value behind the wave front. The width of the annealing region and the speed of its propagation depend on the characteristics of the sample and on the defect density.

However, in pure form, an autowave of annealing is realized only in an infinite sample, which is at absolute zero temperature, when spontaneous thermal annealing is completely “frozen”. Besides, it is assumed that the autowave is initiated infinitely far from the place of observation.

When a sample of finite size is annealed, the autowave regime can be realized as a part of inhomogeneously developing annealing, since transient processes, related to the initiation of an

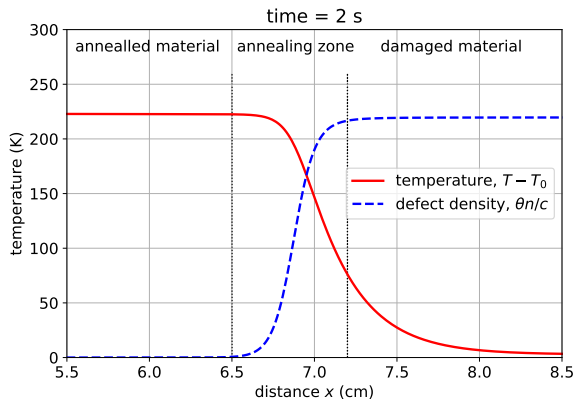


Figure 1. Schematic of the annealing wave front, propagating from the annealed material to the damaged material. Annealing predominantly takes place in the area indicated as “annealing zone”.

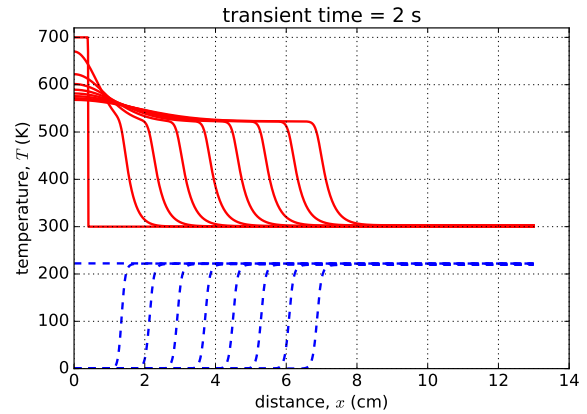


Figure 2. Annealing propagation fronts at 0.2 s time intervals for temperature (top) and defect density (bottom) in a sample of length $L = 13$ cm. Parameters of initial heating are $\Delta T = 400$ K and $\Delta x = 4$ mm.

autowave, or the influence of boundaries (sample surfaces), are always present in this case. It is therefore important to compare the sizes of the sample with the characteristic sizes of the annealing regions, of the wave initiation, and of the influence of the boundary regions. This comparison is especially indispensable at sample temperatures other than absolute zero, when the annealing wave is damped as a result of spontaneous annealing, which occurs throughout the sample volume: the defect density decreases, the influence of the thermo-concentration feedback weakens (reduces), and the criterion for the development of the autowave regime ceases to be satisfied. Thus, minimizing the annealing time of defects of a finite sample with given sizes at a nonzero initial temperature becomes nontrivial and requires the use of numerical methods.

2. Formulation of the problem and basic equations

Consider a sample having the form of a slab of thickness L , which is located in the region $0 < x < L$ and assumed to be infinite in lateral directions (one-dimensional problem). The initial distribution of defects over the volume of the sample is homogeneous and has a density n_0 . The initial temperature of the sample is T_0 everywhere except for a subsurface layer at $x = 0$ with a depth $\Delta x < L$, where the temperature is higher by an amount of ΔT .

Following [4], we take into account that when annealing each defect, an energy, which is approximately equal to the energies of formation of this defect, is released. The released energy is converted into heat and causes an increase in the temperature of the sample. Due to the increase in temperature, the annealing rate also increases. This forms a nonlinear feedback between the temperature and the density of the defects. Due to this feedback and the thermal conductivity of the sample, a self-propagating self-sustaining annealing mode can develop [2].

With this connection in mind, equations for the evolution of the defect density and temperature distributions take the following form

$$\begin{aligned} \frac{\partial n}{\partial t} &= -\frac{n}{\tau}, \\ c \frac{\partial T}{\partial t} &= \kappa \frac{\partial^2 T}{\partial x^2} + \theta \frac{n}{\tau}. \end{aligned} \quad (1)$$

Here c is the volumetric heat capacity and κ is the thermal conductivity of the material; θ is

the energy released as a result of annealing of one defect. The characteristic lifetime of defects, τ , depends, as a rule, on the temperature according to the Arrhenius law:

$$\tau^{-1} = \tau_0^{-1} \exp(-E_a/k_B T), \quad (2)$$

where E_a is the activation energy of annealing, k_B is the Boltzmann constant and τ_0 is a constant depending on material properties. Equations (1) are similar to the governing equations for combustion waves in a premixed solid fuel in a one-dimensional configuration [5].

The problem (1)–(2) is solved subject to the zero-flux boundary conditions:

$$\left. \frac{\partial n}{\partial x} \right|_{x=0} = \left. \frac{\partial n}{\partial x} \right|_{x=L} = 0, \quad \left. \frac{\partial T}{\partial x} \right|_{x=0} = \left. \frac{\partial T}{\partial x} \right|_{x=L} = 0, \quad (3)$$

and initial distributions of defect density and temperature (initial conditions):

$$\begin{aligned} n(t=0, x) &= n_0, & 0 < x < L; \\ T(t=0, x) &= \begin{cases} T_0 + \Delta T, & 0 < x < \Delta x; \\ T_0, & \Delta x < x < L. \end{cases} \end{aligned} \quad (4)$$

The problem (1)–(4) was solved numerically with a Python program, developed and implemented as a part of the research project. In the algorithm employed by the program, a finite difference discretization was performed in space thus yielding a system of coupled nonlinear ordinary differential equations [6], which then were numerically integrated with the `odeint` submodule of the Python's `Scipy` package [7]. The implemented solution method was verified by comparing results obtained by varying the spatial mesh size and by using different temporal integration algorithms. Additionally, for the homogeneous problem (see discussion in the next section) the results of numerical calculations were verified against analytical solutions.

For the sake of comparison with results presented in [3, 8], values of the model parameters, corresponding to aluminium, were used in our calculations, i.e. $E_a = 0.55$ eV, $\theta = 5.4$ eV, $\tau_0 = 10^{-7}$ s, $c = 2.57 \times 10^6$ J/K m³ and $\kappa = 2.2 \times 10^2$ W/m K.

3. Results and discussion

In this work we define the *annealing time*, t^a , as the time at which the total number of defects in the sample becomes less than 1% of its initial value. We investigate the dependence of the annealing time for different annealing initiation temperatures (ΔT) and at various heating depths (Δx), including (for comparison) case $\Delta T = 0$, in which annealing occurs spontaneously. In this case, due to the symmetry of the problem, the annealing occurs *homogeneously* and the annealing time does not depend on the sample dimensions.

In the case of homogeneous spontaneous annealing, as shown in [8], the defect density decreases and the temperature increases as:

$$\frac{t}{\tau_0} = \text{Ei}\left(\frac{T_a}{T}\right) - \text{Ei}\left(\frac{T_a}{T_0}\right) + \exp\left(\frac{T_a}{T_{\text{tot}}}\right) \left[\text{Ei}\left(\frac{T_a}{T_0} - \frac{T_a}{T_{\text{tot}}}\right) - \text{Ei}\left(\frac{T_a}{T} - \frac{T_a}{T_{\text{tot}}}\right) \right], \quad (5)$$

where $T_a = E_a/k_B$ is the activation energy in kelvin, $T_{\text{tot}} = T_0 + \Theta_0$ (here $\Theta = \theta n/c$ is a temperature increase due to annealing of defects and $\Theta_0 = \theta n_0/c$) and $\text{Ei}(\cdot)$ is the exponential integral function, definition of which can be found, e.g., in [9]. Formula (5) provides an implicit dependence of temperature on time. A similar dependence for the defect density can be obtained by taking energy conservation into account. Indeed, in the process of homogeneous annealing in a thermally isolated system the energy stored in defects is converted to heat, hence $T = T_{\text{tot}} - \Theta$, and (5) can be rewritten as an implicit dependence of defect density on time:

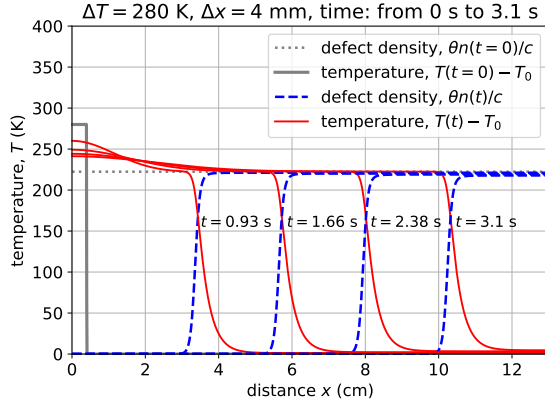


Figure 3. Schematic of annealing wave fronts propagating from the annealed material to the damaged material in the autowave regime.

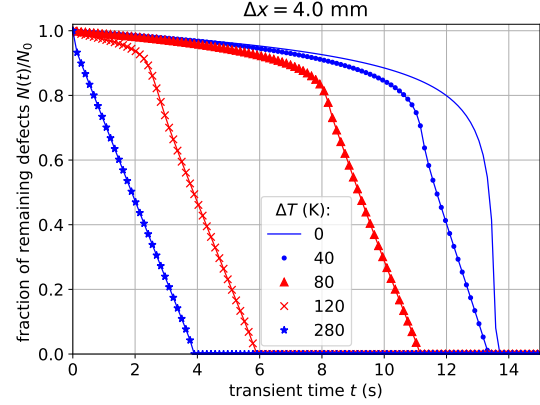


Figure 4. The time evolution of the fraction of remaining defects for different initiating energies.

$$\frac{t}{\tau_0} = \text{Ei} \left(\frac{T_a}{T_{\text{tot}} - \Theta} \right) - \text{Ei} \left(\frac{T_a}{T_0} \right) + \exp \left(\frac{T_a}{T_{\text{tot}}} \right) \left[\text{Ei} \left(\frac{T_a}{T_0} - \frac{T_a}{T_{\text{tot}}} \right) - \text{Ei} \left(\frac{T_a}{T_{\text{tot}} - \Theta} - \frac{T_a}{T_{\text{tot}}} \right) \right]. \quad (6)$$

The annealing time, t^a , can be determined analytically by substituting $\Theta = \Theta_0 \times 1\%$ into formula (6). It follows from (6) that the annealing time decreases with increasing initial temperature and initial defect density. It also decreases with increasing energy released in the process of annealing of one defect, θ . For homogeneous initial distributions of temperature and defect density $T_0 = 300$ K and $n_0 = 6.63 \times 10^{26} \text{ m}^{-3}$, respectively, and for the energy released per one annealed defect $\theta = 5.4$ eV, the annealing time is $t^a = 13.63$ s. This value of the annealing time coincides with the value that was determined numerically in this study using the finite difference method. Since the autowave moves at a constant speed, the annealing rate of the total number of defects per unit area, defined as $R = -dN/dt$, is a constant. This allows us to diagnose the establishment of the autowave regime and determine the propagation velocity of the annealing front using the rate of change of the fraction of the total number of defects, $F = N/N_0$, in time

$$v = -\frac{d}{dt} \int_0^L \frac{n(t, x)}{n_0} dx \approx -L \frac{\Delta F}{\Delta t}. \quad (7)$$

In Fig. 3 we show the evolution of the annealing front in a sample of length $L = 13$ cm with the initial defect density is $n_0 = 6.63 \times 10^{26} \text{ m}^{-3}$. One may observe that, in the autowave regime, defects in the sample anneal at a constant rate. The corresponding time evolution of the fraction of defects remaining in the sample is shown in Fig. 4 for different initiating energies. By using (7) we determined that the speed the annealing front is of $v = 3.18$ cm/s.

The annealing front speed in the autowave regime can also be determined by observing the time required for the front to move through the sample. If we neglect the development time of the autowave regime and the influence of boundaries, then the annealing time in this regime is approximately $t^a = (L - \Delta x)/v$, where v is the annealing propagation speed. Our calculations show that for a localized initial heat distribution at the left boundary of $\Delta T = 280$ K for $\Delta x = 4$ mm, initial defect density $n_0 = 6.63 \times 10^{26} \text{ m}^{-3}$ and $L = 13$ cm, the annealing time is $t^a = 3.85$ s and the annealing propagation speed is $v = 3.27$ cm/s. The results of annealing time calculations for this set of parameters are presented in Figs. 5 and 6.

Alternatively, the annealing propagation speed in the autowave regime can be obtained from

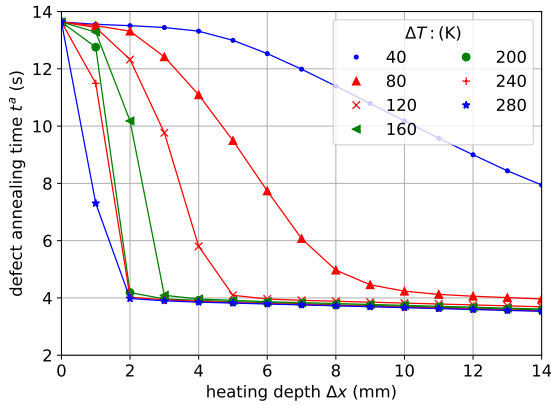


Figure 5. The defect annealing times for different initiating energies.

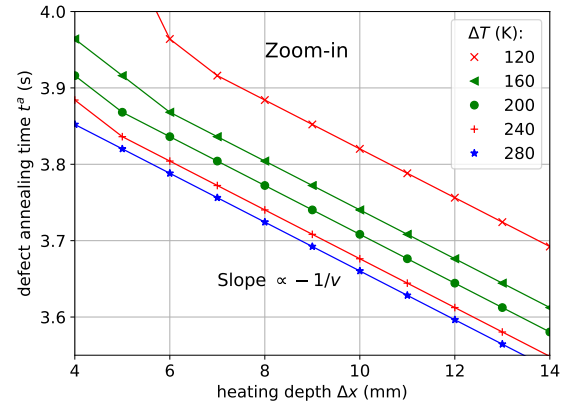


Figure 6. Zoom-in at Δx from 4 mm to 14 mm of Figure 5.

the dependence of the annealing time, t^a , on the heating depth, Δx . Thus, for two different heating depths, Δx_1 and Δx_2 and a fixed ΔT , the propagation speed can be estimated from two corresponding annealing times with the formula, $v = -(\Delta x_2 - \Delta x_1)/(t_2^a - t_1^a)$, where t_2^a and t_1^a are annealing times corresponding to Δx_2 and Δx_1 , respectively. For $\Delta x_1 = 4$ mm and $\Delta x_2 = 14$ mm the annealing times are $t_1^a = 3.85$ s and $t_2^a = 3.28$ s, respectively, for an initiation temperature of $\Delta T = 280$ K. For this configuration, we calculated $v = 3.12$ cm/s.

Therefore, by taking all three estimated values of the annealing propagation speed (v) into account, we find an average value of 3.19 ± 0.08 cm/s (i.e. the spread of speed values in terms of relative standard deviation is within 2.4%).

When annealing is initiated by heating the left boundary of the sample, the annealing occurs in-homogeneously: heat flows from the left boundary to the right and the annealing follows the heat flow. At higher initiation temperatures the defects are annealed faster and for some combinations of parameters the self-propagating annealing wave develops (Figs. 5 and 6).

With the increase in the initiation energy (defined, per unit of surface, as $Q = c\Delta x\Delta T$), the duration and length of the transition regime decreases and tends to zero, an autowave regime appears and displaces the transient mode (Fig. 5). The autowave regime is realized at an earlier time and covers a larger and larger part of the sample. As the autowave regime develops, the annealing time decreases (first quickly and then slowly) and tends to its limit, which corresponds to the time which the autowave initiated at infinity passes the interval $L - \Delta x$ (Figs. 5 and 6).

Furthermore, according to Fig. 5, the influence of the increase in the initiation temperature ΔT is more prominent than the increase in the heating depth Δx . Indeed, at constant initiation energy Q_0 , it is the rise in the initiation temperature and the reduction in the heating depth (rather than the converse) that leads to a decrease in the annealing time. This is due to the fact that the rate of annealing and the accompanying heat release are functions (exponential) of the temperature.

The initiation temperature affects the most strongly the modes in which the autowave formation occurs at the length of the sample. When annealing is realized in a mode close to a hybrid or homogeneous and autowave modes, the autowave regime does not have time to develop or it develops very rapidly. So an increase of Δt at constant energy of initiation does not lead to a decrease in neither the annealing time nor its speed. Conversely, in the autowave regime, there is a slight increase in the annealing time with growth of ΔT .

An increase in the initial defect density leads to a decrease in the annealing time (Fig. 7). This dependence arises from a nonlinear feedback between the temperature and the annealing rate

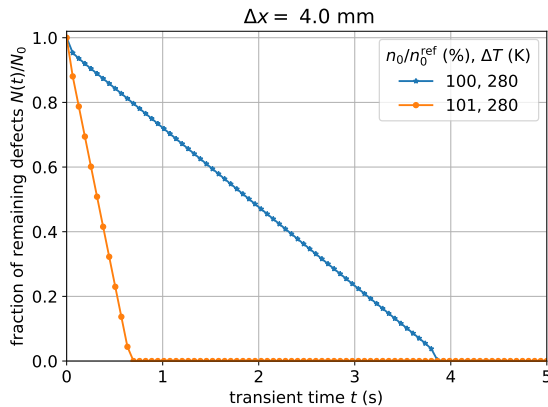


Figure 7. The evolution of the fraction of remaining defects in time for different initial defect densities. Here $n_0^{\text{ref}} = 6.63 \times 10^{26} \text{ m}^{-3}$.

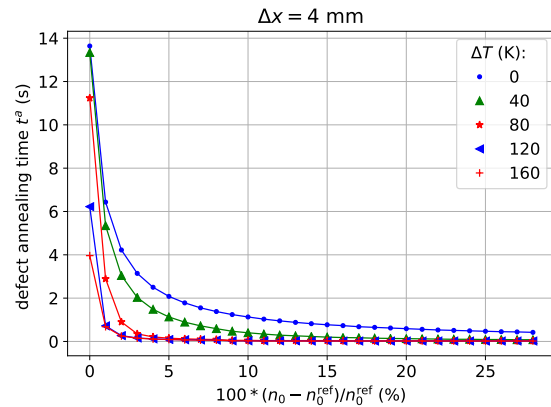


Figure 8. The defect annealing times for different initial defect densities. The reference value is $n_0^{\text{ref}} = 6.63 \times 10^{26} \text{ m}^{-3}$.

of the defects: one can demonstrate that for uniform *isothermal* annealing, this time does not depend on the initial density of the defects. With the dominance of self-propagating annealing, an increase in the initial defect density leads to an increase of the speed of its propagation, as is clearly seen in Fig. 7, as well as to a change in the annealing time. When the initial defect density was increased by one percent, we observed an increase in the annealing speed to $v = 19.08 \text{ cm/s}$. Initiation by a stronger heating pulse intensifies the annealing process and reduces the annealing time even further (Fig. 8).

4. Conclusion

Our calculations have shown that for a sample of a given size (13 cm) and for the parameters used, the annealing time decreases both with an increase in the initiation energy and with an increase in the initial defect density. We have found out that the speed of annealing propagation in the autowave regime is constant, and the time of homogeneous annealing does not depend on the size of the sample. Estimations of the speed of the autowave, performed in three different ways, show a good agreement (the relative standard deviation is within 2.4%).

References

- [1] Bondarenko G G 2016 *Radiation physics, structure and strength of solids* (Moscow: BKL Publishers) (in Russian)
- [2] Selyshchev P A 2014 *Proceedings of the XXIV International Conference Radiation Physics of Solids* ed Bondarenko G G (Moscow: GNU NII PMT) pp 589–594 (in Russian)
- [3] Bokov P M and Selyshchev P A 2016 *IOP Conference Series: Materials Science and Engineering* **110** 012055
- [4] Selyshchev P A 2008 *Self-organization in radiation physics* (Moscow, Izhevsk: R&C Dynamics) (in Russian)
- [5] Weber R O, Mercer G N, Sidhu H S and Gray B F 1997 *Proceedings of the Royal Society of London A: Mathematical, Physical and Engineering Sciences* **453** 1105–1118
- [6] Bokov P M 2017 Finite-difference method for modelling the self-sustained annealing of radiation defects Tech. Rep. RRT-FMR-REP-17001 Necsa
- [7] Jones E, Oliphant T, Peterson P *et al.* 2001– SciPy: Open source scientific tools for Python [Online; accessed 2018-06-09] URL <http://www.scipy.org/>
- [8] Selyshchev P A and Bokov P M 2018 *Nonlinear Systems, Vol. 2: Nonlinear Phenomena in Biology, Optics and Condensed Matter* ed Archilla J F R, Palmero F, Lemos M C, Sánchez-Rey B and Casado-Pascual J (Cham: Springer International Publishing) pp 283–314 ISBN 978-3-319-72218-4
- [9] Press W H, Teukolsky S A, Vetterling W T and Flannery B P 1992 *Numerical Recipes in C (2nd Ed.): The Art of Scientific Computing* (New York, NY, USA: Cambridge University Press) ISBN 0-521-43108-5